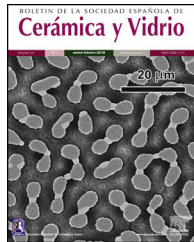




ELSEVIER

BOLETIN DE LA SOCIEDAD ESPAÑOLA DE Cerámica y Vidrio

www.elsevier.es/bsecv



Sintering behaviour of a clay containing pyrophyllite, sericite and kaolinite as ceramic raw materials: Looking for the optimum firing conditions

Pedro J. Sánchez-Soto^a, Eduardo Garzón^{b,*}, Luis Pérez-Villarejo^c, Dolores Eliche-Quesada^d

^a Instituto de Ciencia de Materiales de Sevilla, Centro Mixto Consejo Superior de Investigaciones Científicas (CSIC)-Universidad de Sevilla, c/Américo Vespucio 49, Edificio cicCartuja, 41092 Sevilla, Spain

^b Departamento de Ingeniería, Universidad de Almería, 04120 La Cañada de San Urbano s/n, Almería, Spain

^c Departamento de Ingeniería Química, Ambiental y de los Materiales, Escuela Politécnica Superior de Linares, Universidad de Jaén, Campus Científico-Tecnológico Cinturón Sur s/n, 23700 Linares, Jaén, Spain

^d Departamento de Ingeniería Química, Ambiental y de los Materiales, Escuela Politécnica Superior de Linares, Universidad de Jaén, Campus Las Lagunillas s/n, 23071 Jaén, Spain

ARTICLE INFO

Article history:

Received 12 May 2021

Accepted 17 September 2021

Available online 7 October 2021

ABSTRACT

The sintering behaviour of a pyrophyllite clay has been investigated. The mineralogical composition by X-ray diffraction (XRD) of this sample was ~35 wt.% pyrophyllite, ~25 wt.% sericite/illite, ~15 wt.% kaolinite and ~20 wt.% quartz. The chemical composition was consistent with these results, with a total flux content of 4.18 wt.%. Prismatic bars were prepared by dry pressing using this sample and fired in the range 800–1500 °C with 0.5–5 h of soaking times. Sintering diagrams were obtained using the results of linear firing shrinkage, water absorption capacity, bulk density and apparent porosity determined in the ceramic bodies as a function of firing temperatures. It was found a trend of slight variations of bulk density values firing in the range 1000–1150 °C, with marked decreases of these values for these bodies fired at 1200 °C and 1300 °C. The temperature of maximum bulk density was determined as ~1200 °C and the vitrification temperature was ~1300 °C where the apparent porosity becomes almost zero. The vitrification process of the pyrophyllite clay sample was investigated using a method previously described in the literature, which considered an Arrhenius approach under isothermal conditions and a first order kinetic. It was determined an activation energy (E_a) of ~45 kJ/mol with a linear correlation coefficient of 0.998. The relative rates of vitrification were calculated. It was found that the contribution of vitrification due to the heating was relatively small compared to the vitrification during soaking. Mullite and quartz are forming the ceramic bodies besides a vitreous or glassy phase. The thermally treated pyrophyllite clay showed a dense network of rod-shaped and elongated

Keywords:

Pyrophyllite

Sericite

Sintering

Vitrification

Activation energy

Mullite

* Corresponding author.

E-mail address: egarzon@ual.es (E. Garzón).

<https://doi.org/10.1016/j.bsecv.2021.09.001>

0366-3175/© 2021 SECV. Published by Elsevier España, S.L.U. This is an open access article under the CC BY-NC-ND license (<http://creativecommons.org/licenses/by-nc-nd/4.0/>).

needle-like crystals, being characteristic features of mullite as a dense felt. The vitrification rate equation, as deduced in this study by first time, can be a useful tool to estimate the optimum firing conditions of the pyrophyllite clays applied as ceramic raw materials.

© 2021 SECV. Published by Elsevier España, S.L.U. This is an open access article under the CC BY-NC-ND license (<http://creativecommons.org/licenses/by-nc-nd/4.0/>).

Sinterización de una arcilla que contiene pirofilita, sericita y caolinita como materia prima cerámica: buscando las condiciones óptimas de cocción

R E S U M E N

Palabras clave:

Pirofilita
Sericita
Sinterización
Vitrificación
Energía de activación
Mullita

En el presente trabajo se ha estudiado el comportamiento de sinterización de una arcilla con pirofilita que posee una composición mineralógica (% en peso), deducida por difracción de rayos X, de ~35% de pirofilita, ~25% de sericita/illita, ~15% de caolinita y ~20% de cuarzo. La composición química fue consistente con estos resultados y mostró un contenido total de fundentes de 4,18% en peso. Se prepararon probetas conformadas como barras prismáticas mediante prensado uniaxial, en seco, de la muestra original para estudiar su comportamiento en cuanto a sinterización en el intervalo de temperaturas 800–1.500 °C, con tiempos de permanencia desde 0,5 a 5 h. Se obtuvieron los diagramas de sinterización utilizando los resultados de contracción lineal por cocción, capacidad de absorción de agua, densidad y porosidad aparente determinadas en las probetas tratadas térmicamente en función de la temperatura. Se ha encontrado una tendencia a presentar variaciones no muy importantes de los valores de densidad de las probetas cerámicas en el intervalo 1.000–1.150 °C, con un marcado descenso de estos valores cuando se trataron térmicamente a 1.200 °C y 1.300 °C. La temperatura del máximo de densidad se produce a ~1.200 °C y la temperatura de vitrificación ~1.300 °C, a la cual la porosidad aparente llega a alcanzar valores casi nulos. El proceso de vitrificación de esta arcilla con pirofilita se ha investigado utilizando una metodología descrita en la bibliografía que considera una aproximación de tipo Arrhenius, bajo condiciones isotérmicas, y una cinética de primer orden. Con la aplicación de dicha metodología se determinó una energía de activación $E_a \sim 45 \text{ kJ/mol}$ y un coeficiente de correlación lineal de 0,998. Se calcularon las velocidades relativas de vitrificación durante el tiempo de permanencia a varias temperaturas. Con la realización de este análisis se encontró que la contribución de la vitrificación debida al tratamiento térmico es relativamente pequeña comparada con la vitrificación originada por el tiempo de permanencia a cada temperatura. En las fases cristalinas, la mullita y el cuarzo constituyen los cuerpos cerámicos obtenidos, además de la fase vítreos. Esta materia prima sometida a tratamiento térmico dio lugar a un denso entramado reticular de cristales alargados, formando agujas características, de mullita como denso fieltro. La ecuación de velocidad de vitrificación que se ha deducido en este estudio, por primera vez, puede ser una herramienta de cierta utilidad para estimar las condiciones óptimas de cocción al emplear este tipo de arcillas con pirofilita y sericita como materias primas cerámicas.

© 2021 SECV. Publicado por Elsevier España, S.L.U. Este es un artículo Open Access bajo la licencia CC BY-NC-ND (<http://creativecommons.org/licenses/by-nc-nd/4.0/>).

Introduction

Sintering studies of clay materials

The high-temperature structural applications of ceramic materials based on raw clays involve the knowledge of the sintering behaviour or vitrification process. An early work by Norris et al. [1] proposed an experimental method for the study of vitreous pottery bodies, the so-called “range curves” and the determination of a “temperature of vitrification”, where porosity becomes almost zero. Vitrification is the result of heat treatment and fusion during which a glassy, or non-crystalline

phase, is produced [1–5]. Thus, a progressive reduction in the porosity of the clay material is achieved. In the case of clay-based ceramics, such as triaxial whiteware bodies (composed of clay, kaolin, quartz and alkali or alkali-earth feldspars) feldspars start to melt at about 1000–1100 °C depending on its alkali content [6–8]. The vitrification range is the temperature interval between the temperature at which a ceramic material starts to fuse and the temperature at which the ceramic commences to deform by melting. Vitrification is complete when maximum density and zero porosity are achieved without deformation. Thus, a semiempirical attempt to analyse vitrification process has been proposed by Bogahawatta and Poole [2] to study ceramic raw materials constituted by clays.

It was based on experimental observations of apparent porosity (open porosity) and density, calculating heat treatment and optimum conditions of firing, and an Arrhenius analysis involving the temperature dependence of the vitrification rate. These authors developed a thermal processing equation and the so-called vitrification activation energy can be obtained [2]. Using this approximation, Faieta-Boada and McColm [3] performed a preliminary analysis of the thermal behaviour of an industrially used clay mineral from Ecuador (containing ~35 wt.% of a “disordered kaolin phase” according to these authors).

Other authors, for instance Monteiro and Vieira [9] studied the solid state sintering of clay particles (kaolinite) using a model of close packed discs of a few micrometers (diameter <2 µm) and nanoscale thickness (<0.1 µm). These authors described the nanoscale solid state sintering of clay particles and nanoscale sintering mechanism for clay particles [9]. This particular model was proposed to explain a much more efficient sintering process for clay minerals than the classical spherical particle model [10], with specific characteristics of high contact surface area, lower porosity and nanoscale pores. Freyburg and Schwarz [11] studied the influence of the clay type on the pore structure and microstructural development of structural ceramics. They investigated 51 clayey raw materials of different geological classifications and distinguished four clay types: kaolinitic, illitic-kaolinitic, mixed layer and carbonate-containing clays. The results of this investigation indicated that the sintering behaviour of these four clay types showed significant differences.

Vitrification of illitic clay via phase and microstructural changes, has been investigated from 800 to 1250 °C by Wattanasiriwech et al. [12] using a sample clay (Ipoh, Malaysia) containing illite (~23 wt.%), kaolinite (~41 wt.%), quartz (~30 wt.%), hematite (~3 wt.%) and rutile (~1 wt.%), with 2.90 wt.% of K₂O. Firing shrinkage of this illitic clay showed that densification of the body should starts around 900 °C and was highly achieved at 1200 °C. According to the findings of these authors, illite acted as superb melting agent in the natural mineral mixture upon elimination of pores in the matrix. These authors concluded that the diffusion of potassium was confirmed by the formation of crystals, with rectangular shape, on the surface of the ceramic body, being close to “the glassy pool of illite relicts”.

The variation of linear shrinkage and determination of the vitrification curve of stoneware tiles (red porcelain) have been studied by Melnick et al. [13]. They used a dilatometric method with a dwell time of 1 h at the final temperature (1100 °C). The sample was a mixture (50 mass%) of clay-siltstone shale and capping siltstone. The predominant clay mineral was kaolinite (49.8 mass%), with illite (10 mass%) and quartz (30.3 mass%), and hematite (7.3 mass%). On the other hand, an investigation of the sintering mechanisms of kaolin-muscovite mixtures (0–25 mass% muscovite) has been performed by Lecomte-Nana et al. [14] based on non-isothermal measurements. The raw materials were reference kaolin (sample KGa-1, 96 mass% kaolinite) and a muscovite sample (99 mass%, Bihar, India). When muscovite content was >10 mass%, the densification resulted of the same mechanism as the kaolin up to 1300 °C, and above this temperature up to 1500 °C, densification was also the consequence of “dissolution-limited liquid sintering”

with an activation energy of <250 kJ/mol. However, vitrification rate of raw clays containing pyrophyllite have not been reported until now.

Pyrophyllite and pyrophyllite clays with sericite and kaolinite

Pyrophyllite and pyrophyllite clays with sericite and kaolinite have been investigated as raw materials applied for ceramics and refractories along years [15–20]. Pyrophyllite is a relatively rare mineral, found in metamorphic rocks [19]. Sánchez-Soto and Pérez-Rodríguez [17,18] reviewed the precedent investigations concerning this kind of raw materials and their applications. In this sense, it is of particular interest the raw materials composed of sericite/illite, kaolinite, pyrophyllite and, sometimes, quartz. Zaykov and Udachin [16] studied pyrophyllite raw materials in the sulphide-bearing areas of the Urals. The sintering capacity was determined for quartz-pyrophyllitic and quartz-sericite-pyrophyllitic raw materials obtained from these deposits. Bentayeb et al. [19] presented a mineralogical study of pyrophyllite (from Morocco), showing the presence of mica and quartz. Further study by Bentayeb et al. [20] showed a more complete characterisation of this pyrophyllite sample (59.0 mass% of pyrophyllite, 11.7% of mica-like and 27.6 mass% of quartz) and its possible applications. Sánchez-Soto et al. [21] reported the results of an investigation on the influence of mechanical and thermal treatments on raw materials containing pure pyrophyllite and pyrophyllite clays with kaolinite and sericite/illite.

The use of high-sericite pyrophyllite in vitreous bodies was studied in a pioneering work by Emrich [22]. The effect of pyrophyllite on vitrification and on physical properties of triaxial porcelain has been investigated by Mukhopadhyay et al. [23]. These authors further studied the effect of pyrophyllite on the mullitisation in the same system [24]. The sample was a raw pyrophyllite with some quartz. Mukhopadhyay et al. [25] consider that the use of pyrophyllite as ceramic raw material is not yet widely accepted. Incorporation of pyrophyllite as a replacement of china clay in a conventional whiteware ceramic body resulted in lowering its vitrification temperature. Then, it can be deduced that this raw pyrophyllite is not a pure sample but a sericitic/muscovitic sample [25].

Talidi et al. [26] reported the application of pyrophyllite clay in the processing of tubular ceramic as support for microfiltration membrane. It was a subject investigated by Ha et al. [27] preparing diatomite-pyrophyllite porous membranes and by Ha et al. [28] preparing porous composite support layers based on alumina-coated pyrophyllite sintered at 1400 °C/1 h. Interestingly, a proposal for the formulation of high-quality ceramic “green” materials, with traditional raw materials mixed with Al-clays (Palaeozoic weathered shales), has been reported by González et al. [29]. These authors used Al-clays containing kaolinite, mica (illite-sericite) and pyrophyllite, with minor amounts of quartz and other minerals mixed with the marls traditionally used in ceramic production facilities in south Spain to fabricate structural ceramic materials. The presence of very fine-grained mica (10–20 µm sericite) in these raw clays, with low quartz and iron contents, makes them especially interesting in ceramic manufacture. It can be also mentioned that illite is one of the major component of clays used in

traditional ceramics, for instance to be applied for the production of bricks, tiles, plates and stoneware tiles [30,31].

It should be remarked the important contribution of several research Institutes of CSIC and University Departments, in particular the ICV (CSIC) at Madrid, with a proposal of sericite clays (without or with pyrophyllite) as new ceramic raw materials [32–34]. The sericite clays produce ceramic materials with very high mullite content at relatively low temperatures by heating, with formation of a very reactive glassy phase and an exceptional firing range [17,18,31–39]. Furthermore, Wang et al. [40] used sericite to induce textural structures in the preparation of emulsion-templated high-porosity mullite ceramics. Hsiao et al. [41] have studied the synthesis of analcime from sericite and pyrophyllite. It should be noted here that a previous systematic investigation on these raw materials was conducted by Galán Huertos and Espinosa de los Monteros [42], studying the deposits of raw kaolins in Spain, some of them containing sericite and pyrophyllite. These raw materials have been named in Spain as “white earths” or “white shales” taking into account its colour in the environments of local deposits and, according to precedent studies [36], they are also named as kaolinitised shales, illitic-kaolinitic clays, aluminium shales, sericitic shales, sericite clays or sericites, although some of them contain pyrophyllite.

It is important to mention that an investigation by Sule and Sigalas [43] reported the effect of temperature on mullite synthesis from pyrophyllite and α -alumina by spark plasma sintering. The pyrophyllite powder (Ottosdal, South Africa) contained 1.26 mass% of K_2O and Na_2O . The presence of sericite in this sample was not mentioned, but according the reported chemical analysis, this sample was a pyrophyllite with sericite. The glassy phase originated by the impurities of this sample influences the sintering behaviour because spark plasma sintering can induce rearrangement of particles. Thus, the majority of the samples considered as “pyrophyllite” in the literature are, in rigour, sericite-pyrophyllite or kaolinite-sericite-pyrophyllite raw clay materials, sometimes with quartz, and other minerals (feldspars, rutile, iron oxide, etc.) although in relative low proportion.

However, despite all these previous studies and interesting reports on thermal properties, the sintering or vitrification behaviour of pure pyrophyllite and pyrophyllite clays containing sericite and kaolinite has not been yet studied, in particular with an analysis of firing conditions. Thus, the aim of the present work was to investigate the sintering behaviour of such as raw clay materials. For this purpose, a raw pyrophyllite clay sample has been selected. Vitrification has been analysed using the method described by Bogahawatta and Poole [2], which considered an Arrhenius approach involving the temperature dependence of the vitrification rate.

Material and methods

Sample used in this study

A sample of raw pyrophyllite located near Cáceres (south west Spain), supplied by Alicún Prospecciones S.L., has been selected for the present study. The as-received clay sample

(named as “Pizarrilla”) was slightly ground and sieved to pass 200 μm . Then, the sample was firstly air-dried (24 h) and secondly the powder was dried at 110 °C for 24 h.

Techniques of characterisation

The particle size of the sample was determined by sedimentation, following the method described by Galán Huertos and Espinosa de los Monteros [42].

The chemical composition of the raw sample was determined by Atomic Absorption Spectroscopy (AAS). The sample was prepared by acid dissolution using a chemical procedure taking into account the presence of pyrophyllite, which is not dissolved in tri-acid water solutions ($\text{HF}-\text{HClO}_4-\text{HCl}$) [44,45]. The equipment was a Perkin-Elmer, model 703, using air or dinitrogen oxide-acetylene flame.

The alkaline elements were determined by Flame Photometry, using an equipment Evans Electroelenium. The LOI (“Loss On Ignition”) was determined by thermal treatment at 1000 °C for 1 h using an alumina crucible and 1.000 g of sample.

The crystalline phase analysis was performed by X-ray diffraction (XRD). The powdered samples, previously ground using an agate mortar and pestle, were scanned using random preparations in an X-ray diffractometer Siemens equipment, model D-5000, using Ni-filtered $\text{CuK}\alpha$ radiation and graphite monochromator. This equipment operated at 40 kV and 20 mA. In the case of the raw pyrophyllite samples, the mineralogical composition by XRD was estimated using the classical methods proposed by Schultz [46] and Biscey [47], with the modifications provided by several authors [36,42].

The raw pyrophyllite and selected thermal treated materials were examined by Scanning Electron Microscopy (SEM) after coating the samples with a thin layer of gold by sputtering. The equipment for SEM examination was a JEOL JSM 5400 microscope with an Energy Dispersive X-ray Spectroscopy (EDS) system Link ISIS Pentafet Oxford. The thermal treated materials were studied by SEM-EDS in fresh fractured surfaces and after previous etching with aqueous diluted HF (20 wt.%) to remove the glassy phase.

Firing properties. sintering or vitrification diagrams

Starting from the powdered pyrophyllite sample, pressed bodies were prepared as prismatic bars by uniaxial dry pressing, using ~5 wt.% of deionised water, at 150 MPa. These prismatic bars were air-dried (24 h) and then treated at 60 °C for 4 h. They were fired at 8 °C/min (480 °C/h) to selected temperatures in the range 800–1500 °C using an electric laboratory furnace, with SiC heating elements, for 0.5–5 h of soaking times at each temperature and then furnace cooled.

The linear firing shrinkage of the fired prismatic bars was measured with a calliper. Water absorption capacity, bulk density and apparent porosity (open porosity) of these bars were measured by the Archimedes immersion technique, using deionised water as liquid medium, saturation for 24 h and boiling in deionised water for 2 h, according to the Spanish standards [32,37,42,48]. These results, in triplicate measurements, were of interest to construct the sintering or vitrification diagrams [1], showing the evolution of these

properties as a function of firing temperatures and soaking times. Further characterisation analyses were also performed concerning the high-temperature phases and microstructures using XRD and SEM-EDS.

Sintering analysis: application of a previous model of vitrification behaviour of clays

The analysis of optimum firing conditions for the clay pyrophyllite sample is based on a previous analysis of clays containing kaolinite as an approximation [2,3]. A first order kinetic model is applied to the reactions leading to the sintering behaviour of these clays [49]. The temperature dependence of the rate of sintering (vitrification) can be expressed by the Arrhenius equation as:

$$k = A \exp\left(\frac{-E_a}{RT}\right) \quad (1)$$

where k is the rate of reaction (rate of vitrification), A is a constant, E_a is the activation energy, R is the Boltzmann constant and T is the absolute temperature. Redfern [49] studied the thermal decomposition of kaolinite (purified sample supplied by English China Clay Ltd.) and showed that the time required to attain a certain degree of vitrification (t) under isothermal conditions is proportional to $1/k$, i.e., $t=c/k$ where c is a constant. Therefore, from Eq. (1)

$$\ln t = \left(\frac{E_a}{RT}\right) - \ln A' \quad (2)$$

where $A' = A/c$. Consequently, a plot of $\ln t$ versus $1/T$ gives E_a/R as the slope.

The rate of vitrification of a clay at a temperature above 850°C (i.e., incipient vitrification) relative to that at 850°C was considered to be a measure of the overall rate of vitrification at that particular temperature. Therefore, if k_t is the rate of vitrification at $t^\circ\text{C}$ relative to that 850°C (1123 K), Eq. (2) reduces to

$$\ln k_t = \frac{E_a}{R} \left[\frac{1}{1123} - \frac{1}{t+273} \right] \quad (3)$$

Isothermal firing trials can be performed at different temperatures by varying the soaking period. The soaking period corresponding to the optimum degree of vitrification, as shown by the critical changes in properties, was used in the construction of $\ln t$ -reciprocal temperature or Eq. (2) plots. Then, the exponential factor determined for the plot was used in Eq. (3) to calculate the relative rates of vitrification at different firing temperatures. If k_t is the relative rate of reaction (degree of vitrification), as pointed out above, of a clay body at $t^\circ\text{C}$ ($t+273=T$ in K), then the degree of vitrification (V_{heating}) attained during heating, is given by

$$V_{\text{heating}} = \int_{h_0}^h k_t dh$$

where h denotes time and $h-h_0$ is considered the time interval during which temperature was raised from T_0 (1123 K) to

Table 1 – Particle size analysis of the raw pyrophyllite sample.

Size (μm)	wt.%
>200	11.1
200–50	4.2
50–2	62.9
<2	21.8

the maximum firing temperature T (K) at a constant rate. The degree of vitrification attained during soaking is given by

$$V_{\text{soaking}} = k_t \times h_s$$

where h_s is the soaking time.

The overall degree of vitrification (V_{total}) attained during heat treatment of the clay body, according to a fixed firing schedule, is thus given by $V_{\text{total}} = V_{\text{heating}} + V_{\text{soaking}}$ or

$$V_{\text{total}} = \int_{h_0}^h k_t dh + k_t x h_s$$

Results and discussion

Characterisation of the pyrophyllite clay sample

A previous characterisation of the pyrophyllite clay used in the present study has been carried out. Table 1 includes the particle size analysis of this sample. These results indicate that its texture is silt-clayey, with ~22 wt.% of grain sizes $<2\text{ }\mu\text{m}$ (clay fraction) and more than 80 wt.% of grain sizes $<50\text{ }\mu\text{m}$.

The mineralogical composition deduced by XRD (Fig. 1) of this sample indicates ~35 wt.% pyrophyllite, ~25 wt.% illite-sericite, ~15 wt.% kaolinite, with ~20 wt.% quartz and other minor minerals, such as feldspar. A separate analysis by XRD following the procedure described by Wiewióra et al. [50] demonstrated that the polytypic structure of pyrophyllite mineral is triclinic (1Tc).

The results of chemical analysis of this sample by AAS are presented in Table 2. The pyrophyllite clay is constituted mainly by SiO_2 (58.88 wt.%) and Al_2O_3 (30.25 wt.%), with minor amounts of Fe_2O_3 (0.64 wt.%) and TiO_2 (1.41 wt.%). The amount of alkaline elements ($\text{Na}_2\text{O} + \text{K}_2\text{O}$) is 1.64 wt.%. The LOI is 6.82 wt.%, which is associated to the dehydroxylation of phyllosilicates, mainly kaolinite and pyrophyllite. These chemical results are consistent with the mineralogical composition (Fig. 1). Furthermore, taking into account the chemical elements on a calcined basis (Table 2), there is 63.17 wt.% of SiO_2 and 32.47 wt.% of Al_2O_3 a RO content ($\text{CaO} + \text{MgO}$) of 0.23 wt.% and R_2O content ($\text{Na}_2\text{O} + \text{K}_2\text{O}$) of 1.64 wt.%. The total flux content ($\text{RO} + \text{R}_2\text{O} + \text{Fe}_2\text{O}_3 + \text{TiO}_2$) is equal to 4.18 wt.%. It will contribute to form a vitreous or glassy phase by progressive heating [39]. Bogahawatta and Poole [2] studied several kaolinitic clay samples with RO and R_2O contents ranging from 0.91 to 2.86 wt.% and 0.40 to 1.58 wt.%, respectively. The total flux content of these clay samples was in the range 16.31–21.43 wt.% higher than the clay sample studied here.

According to the present results, the content of phyllosilicates in this pyrophyllite clay is ~75 wt.% and shows silico-aluminous chemical characteristics, with a relative low

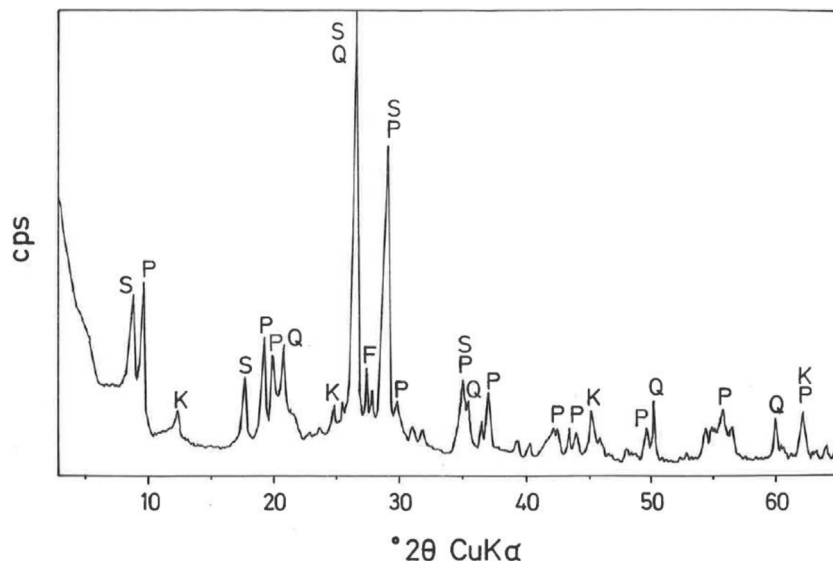


Fig. 1 – XRD diagram of the raw pyrophyllite clay sample. P = pyrophyllite; S = sericite/illite; K = kaolinite; Q = quartz; F = feldspar.

Table 2 – Chemical analysis by AAS of the raw pyrophyllite sample (results in wt.%). “LOI” is “loss on ignition” or weight loss after thermal treatment at 1000 °C for 1 h. “Calcined sample” are the chemical analysis calculated taking into account the LOI.

	SiO ₂	Al ₂ O ₃	Fe ₂ O ₃	TiO ₂	MgO	CaO	Na ₂ O	K ₂ O	LOI	Total
Raw sample	58.88	30.25	0.64	1.41	0.17	0.06	0.24	1.40	6.82	99.87
Calcined sample	63.17	32.45	0.68	1.51	0.18	0.06	0.25	1.50	–	99.80

iron content. Besides this, and considering the low grain size, this sample can be considered as a pyrophyllite clay with sericite. The sericite clays studied by several authors along years [17,18,29,32–39] are characterised, from a mineralogical point of view, by fine grained sericite, presence of kaolinite and/or pyrophyllite in variable proportions and a relative low or very low quartz content.

Fig. 2(a, b) shows two selected SEM images of the raw pyrophyllite clay sample. The SEM observations indicated the presence of stacking layers, with some large flat morphologies, some book-like structures and irregular and flaky particles, sometimes forming aggregates, associated to phyllosilicates. Crystalline grains are observed, which are associated to quartz. EDS analysis (Fig. 2c) is consistent with the presence of phyllosilicates (Al, Si, K), some of them containing K (sericite/illite) and quartz particles, where only Si is detected.

Thermal behaviour: sintering diagrams

The linear firing shrinkage (LFS, %), water absorption capacity (WAC, %), bulk density (BD, g/cm³) and apparent or open porosity (AP, %) are parameters of interest to construct the sintering diagrams (Figs. 3 and 4) according to Norris et al. [1], which correspond to the thermal behaviour of the pyrophyllite sample prepared as pressed prismatic bars. These diagrams allow investigate the thermal evolution of all these parameters as a function of heating temperatures and soaking times. It has been selected the results corresponding to 4 h of soaking time,

although results of 1 h of soaking time for 1200 °C and 1300 °C have been also plotted. The results of Fig. 3 indicate that there is an increase of LFS as increasing firing temperature up to a maximum value at 1200 °C/4 h and 1200 °C/1 h. After this temperature, the sample experimented a progressive decrease of LFS up to 1500 °C. At the same time, WAC of the test samples decreases from 12% at 800 °C/4 h to 3.2% at 1200 °C/4 h, reaching a minimum value of 0.94% at 1300 °C/1 h with an increase to ~3% at 1300 °C/4 h.

The results of Fig. 4 indicate that BD increases from ~2 g/cm³ at 800 °C/4 h to a maximum of ~2.25 g/cm³ at 1200 °C/4 h, and showing a fast decrease up to ~1.7 g/cm³ at 1300 °C/4 h and ~1.55 g/cm³ at 1500 °C/4 h. The evolution of AP (%) demonstrates a progressive decrease from ~24.5% at 1000 °C/4 h to ~5% at 1300 °C/4 h, with a lower value (~2%) at 1300 °C/1 h and showing a slow increase up to ~6.5% at 1500 °C/4 h. Taking into account these results, it can be deduced that after firing at 1200–1300 °C this pyrophyllite clay is sintered. The evolution of BD is of particular interest in the present study following previous investigations [2,3]. Thus, the effects of isothermal soaking (0.5–5 h) on the BD of fired pyrophyllite test samples are presented in Fig. 5. Increasing the soaking period resulted in an increased BD, although it seems that there is an optimum soaking period, with an increase in the degree of heat treatment.

In fact, it can be observed:

- (1) a trend for samples fired at 1000, 1050, 1100 and 1150 °C of slight increases of BD values, and

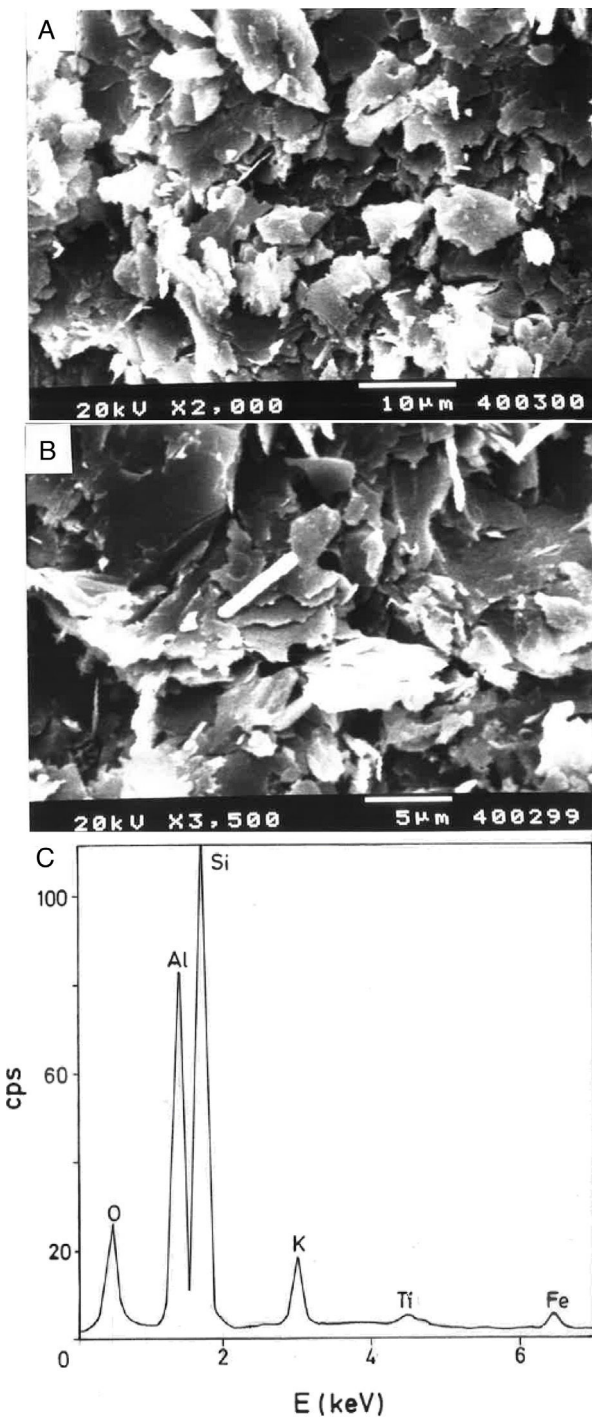


Fig. 2 – Selected SEM micrographs of the raw pyrophyllite clay at low (a) and high (b) magnifications, including an average EDS analysis (c) obtained at low magnification.

- (2) a second trend to marked decrease of BD values for samples fired at 1200 °C and 1300 °C, with a remarkable fall of BD values in samples fired at 1300 °C, starting from 2 h of soaking time.

Thus, heat treatment exceeding an optimum produced a deterioration of BD. Similar trends have been reported in the literature for kaolinitic clay samples after firing [2,3], but it was not reported for pyrophyllite clays until the present research.

According to the previous work of Norrish et al. [1] concerning the study of vitreous ceramic bodies, it can be considered two parameters: (a) the parameter T_v or “vitrification temperature”, defined as the temperature (determined by the sintering diagrams) at which the apparent porosity becomes almost zero, and (b) the parameter T_d or “temperature for maximum bulk density”. In the present study, using the pyrophyllite clay after firing and 4 h of soaking time, from the results presented in Fig. 4, it can be deduced that $T_v \sim 1300^\circ\text{C}$ and $T_d \sim 1200^\circ\text{C}$. It

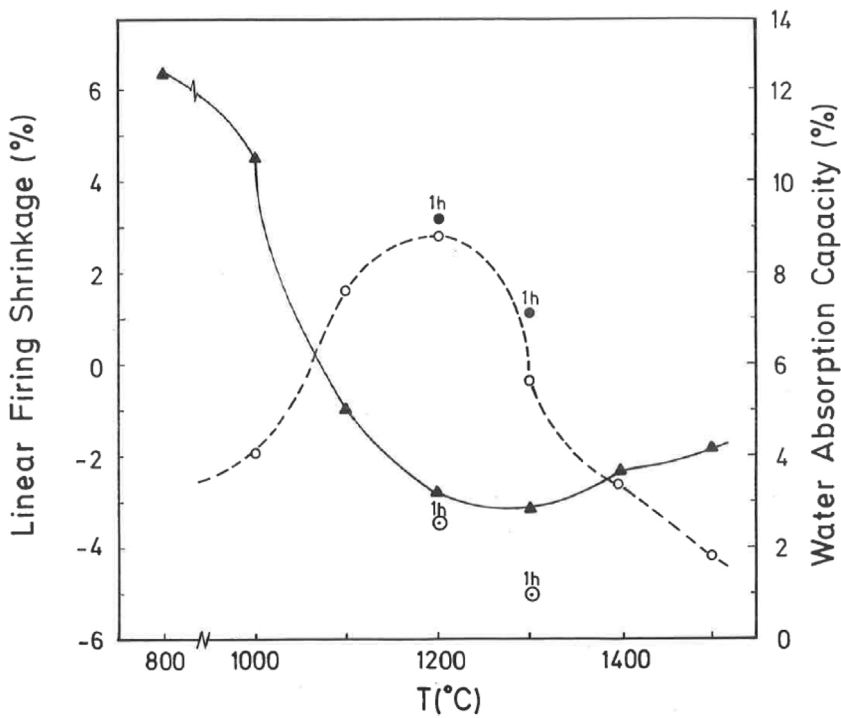


Fig. 3 – Plot of the evolution of linear firing shrinkage (%) and water absorption capacity (%) for the pyrophyllite clay bodies as a function of heating temperature (4 h of soaking time). Some selected points at 1 h of soaking time are included.

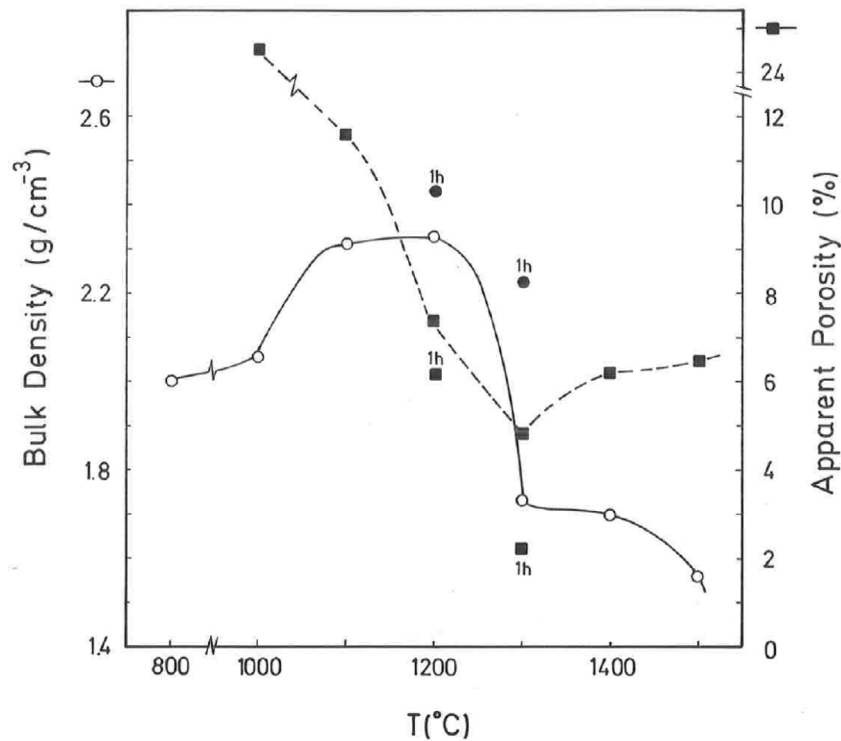


Fig. 4 – Plot of the evolution of bulk density (g/cm^3) and apparent porosity (%) for the pyrophyllite clay bodies as a function of heating temperature (4 h of soaking time). Some selected points at 1 h of soaking time are included.

follows that if vitrification, in some sense, define the sintering it can be considered subsequent processes. Then, the vitrification temperature could be named as “sintering temperature”. Similar values of T_v and T_d (although with soaking times of 1 h) have been reported in a previous study on thermal behaviour

of sericite clays, with or without pyrophyllite, as precursors of mullite materials [38]. Finally, the results presented in Fig. 5 are of particular interest for a deep sintering study of this pyrophyllite clay and an estimation of its optimum firing conditions.

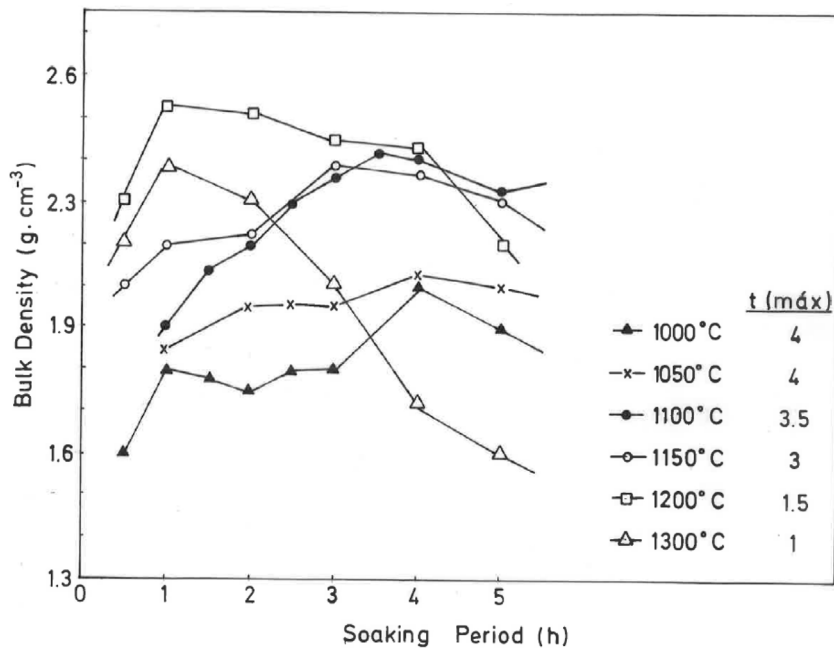


Fig. 5 – Variation of bulk density for the pyrophyllite clay bodies with soaking period (0.5–5 h) at different temperatures (1000–1300 °C). The values of soaking period at the maximum value of BD, $t_{\text{máx}}$, at each temperature are indicated.

Sintering study and analysis using a kinetic model: estimation of optimum firing conditions

The analysis of optimum firing conditions in this sample of pyrophyllite clay is based on a first order kinetics [49] applied to the reactions leading to the sintering behaviour, as was described in the section methods following precedent papers [2,3].

If k_t is the rate of vitrification, then isothermal firing trials can be performed at different temperatures by varying the soaking period. The soaking period corresponding to the optimum degree of sintering (vitrification), as shown by the critical changes in characteristic properties, such as BD in the present case (Fig. 5), is used to the construction of $\ln t$ versus reciprocal temperature plots using Eq. (2). The experimental factor calculated for this plot is used in Eq. (3) to determine the relative rates of vitrification at different firing temperatures.

Taking into account the results presented in Fig. 5, the plot of $\ln t$ versus $1/T$ gives E_a/R as the exponential factor (Fig. 6) with deviation of the straight line from 1200 °C and a correlation coefficient of 0.998. In the present study, the exponential factor E_a/R is determined as 5.422 and the activation energy is $E_a \sim 45 \text{ kJ/mol}$. This value of E_a for the vitrification was not in the range of 74–151 kJ/mol reported by Bogahawatta and Poole [2] in a study on several kaolinitic clays of residual origin. Faieta-Boada and McColm [3], following the same method [2], reported a value of $E_a = 143 \text{ kJ/mol}$ for an Ecuadorian clay (with 35 wt.% of a disordered kaolin phase), suggesting that the controlling mechanism of vitrification is one of viscous flow. In any case, the present work is the first report on the study of sintering of a pyrophyllite clay using this kinetic model and values of exponential factor $E_a/R = 5.422$ and $E_a \sim 45 \text{ kJ/mol}$ have been found.

The previous papers have reported the sintering or vitrification behaviour of kaolinitic clays, as mentioned above [2,3].

Taking into account the exponential factor E_a/R determined from the $\ln t$ versus $1/T$ plot (Fig. 6), the equations presented in methods allow estimate the relative rate of reaction, in this case the degree of vitrification of the pyrophyllite clay body. The analysis is summarised in Table 3. Thus, the relative degree of vitrification for each stage of firing (heating and soaking) can be calculated as

$$V_{\text{total}} = V_{\text{heating}} + V_{\text{soaking}}$$

The analysis of vitrification rate process leads to an equation enabling that optimum firing condition be calculated as follows:

$$V_{\text{total}} = [e^{0.00358 \times 480h}] 0.00358 \times 480 + \left[\frac{e^{4.828}}{e^{5.422/(t+273)}} \right] \times h_s$$

where the parameter V_{total} is the total relative degree of vitrification, r is the heating rate, h is the heating time above 1123 K (850 °C), t is the maximum firing temperature and h_s is the soaking period (Table 3).

It should be noted that Bogahawatta and Poole [2] estimated the error in the calculation of the degree of vitrification for kaolinitic clay bodies. However, Faieta-Boada and McColm [3] did not estimate these errors. The first authors demonstrated that the error involved in the assessment of the total degree of vitrification is relatively insignificant because the contribution of heating to the overall vitrification is small at all temperatures of firing. A similar finding has been deduced in the present study. According to the results of Table 3, the contribution of vitrification due to the heating was relatively small compared to vitrification during soaking.

On the other hand, from the results of Table 3, it can be observed that the total relative degree of vitrification for the pyrophyllite clay is accomplished at 1150 °C, with 3 h of soaking time, and the BD of the body obtained after this thermal treatment is $\sim 2.4 \text{ g/cm}^3$ (Fig. 5). The percentage of

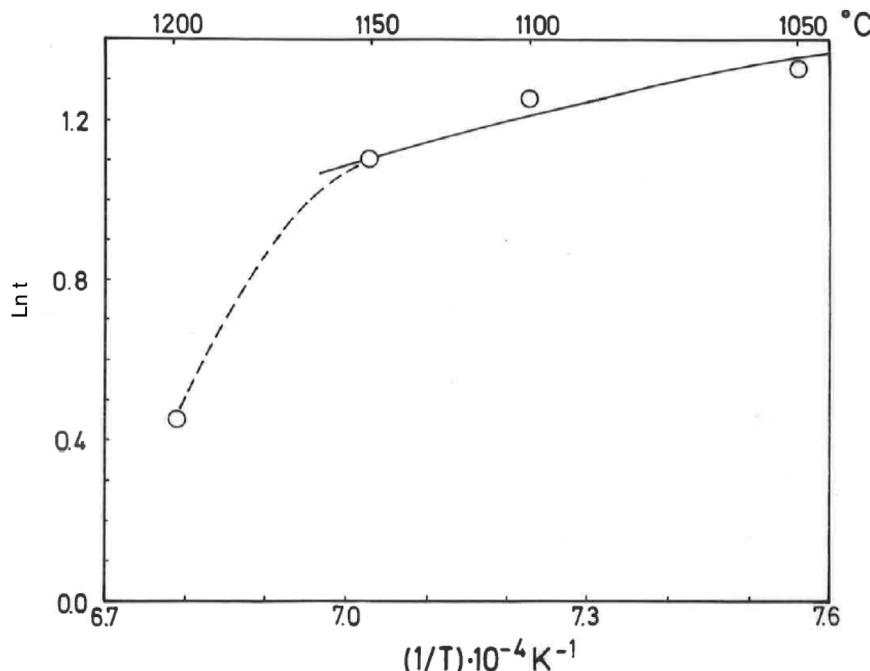


Fig. 6 – Plot of $\ln t$ versus the reciprocal of temperature for isothermal heating of the pyrophyllite clay, following the model proposed by Bogahawatta and Poole [2]. The slope E_a/R of the straight line (three linear points) was determined as 5.422 ($E_a \sim 45 \text{ kJ/mol}$). The correlation coefficient of the straight line is 0.9980.

Table 3 – Calculation of degree of vitrification for the pyrophyllite clay sample subjected to various heat treatments. Firing schedule: $r = 8^\circ\text{C}/\text{min}$ or $480^\circ\text{C}/\text{h}$.

Maximum firing temperature ($^\circ\text{C}$)	Soaking period, h_s (h)	Heating time above 850°C h	Relative degree of vitrification, heating, ^a calculated (arb. units)	Relative degree of vitrification, soaking ^b calculated (arb. units)	Total relative degree of vitrification ^c (arb. units)	% Contribution of heating to overall vitrification
1050	4	0.41	1.2	8.3	9.5	12.6
1100	3.5	0.52	1.4	8.4	9.8	14.6
1150	3	0.62	1.7	8.3	10	17

^a Relative degree of vitrification for each stage of firing: heating; calculated from:

$$V_{\text{heating}} = \int_{h_0}^h k_t dh = \int_{h_0}^h e^{3.58 \times 10^{-3} rh} dh$$

^b Relative degree of vitrification for each stage of firing: soaking; calculated from:

$$V_{\text{soaking}} = \frac{e^{4.828}}{e^{5.422/(t+273)}} \times h_s$$

$$\text{c } V_{\text{total}} = V_{\text{heating}} + V_{\text{soaking}}$$

contribution of heating to overall vitrification for the pyrophyllite clay sample is 17% (Table 3). The total relative degree of vitrification can be calculated according to the equations presented in Table 3, as deduced in the present investigation.

These considerations of the temperature-time relationships for the isothermal heating of this clay has allowed the derivation of empirical equations for the rate of vitrification.

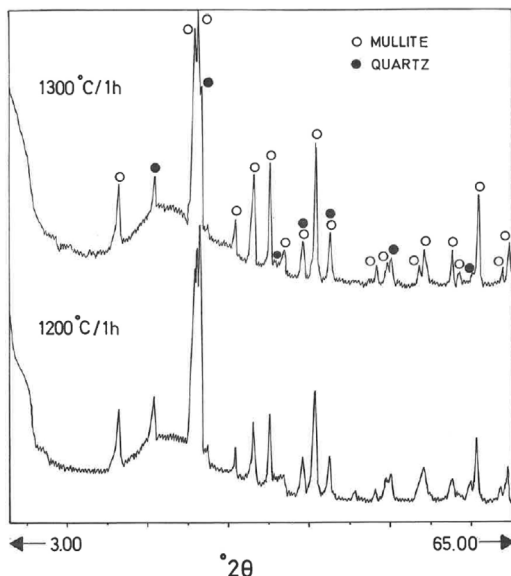


Fig. 7 – XRD diagram of pyrophyllite clay sample bodies after heating at 1200 °C and 1300 °C for 1 h, showing the crystallinity of mullite (formed by thermal decomposition of the layer silicates), the presence of quartz (identified in the raw sample) and the amorphous glassy phase (hump in the XRD background centered at ~22° 2θ).

Finally, as pointed out by the previous studies on this subject [2,3], the vitrification rate equation can be an useful tool for clay manufacturers to calculate the optimum firing cycles, although the first step was under laboratory conditions. Thus, in the present investigation it has been performed using the pyrophyllite clay sample as a ceramic raw material and the achieved result is the equation presented in Table 3. These results are interesting as a first step prior to industrial firing conditions, as mentioned above, for instance in the processing of tubular ceramic support for microfiltration membranes [26] and high porosity mullite ceramics [40] using pyrophyllite clays with or without sericite.

Analysis of crystalline and vitreous phases after firing

The dynamics of clay firing involves the knowledge of crystalline and amorphous phases formed by thermal treatments [51]. In particular, the formation of mullite is a very interesting feature in the present case, as noted in the Introduction section when sericite raw materials were considered. Fig. 7 includes two selected XRD diagrams of the pyrophyllite clay bodies fired at 1200 °C/1 h and 1300 °C/1 h. In both cases, mullite is detected, originated by thermal decomposition of the phyllosilicates (pyrophyllite, kaolinite and illite-sericite) besides residual quartz. A hump in both XRD diagrams at ~22° 2θ is associated to a non-crystalline, amorphous, glassy or vitreous phase [4]. This phase can be removed by chemical attack by using HF. Thus, mullite present in the fired pyrophyllite clay can be observed by SEM (Fig. 8a) forming a dense network of

rod-shaped and elongated needle-like mullite crystals, sometimes as a dense felt, with some relicts of glassy phase, a typical microstructure as found in kaolinitic and sericitic clays and triaxial porcelains [6,32,34,39,52]. It was confirmed by EDS analysis (Fig. 8b), where the relative proportion of Al is higher than Si.

In fact, the chemical attack using HF is quantitative, although quartz crystals are also removed. Hence, a direct gravimetric determination with HF attack and washing the residue (mullite crystals) allowed estimate a mullite amount of $\sim 34 \pm 2$ wt.% in the pyrophyllite clay after firing at 1300 °C/1 h. Then, the relative proportion of quartz and vitreous phase must be ~ 67 wt.%. Quartz content was estimated as ~ 20 wt.% by XRD (see above mineralogical analysis), hence the amount of vitreous phase is estimated as ~ 47 wt.%. In other words, the crystalline (mullite and quartz) and vitreous phase are in $\sim 1:1$ proportion in the pyrophyllite clay body fired at 1300 °C/1 h. However, the proportion of vitreous phase will increase as increasing temperature and soaking time, with deformations in the ceramic bodies, as observed in Fig. 5. The theoretical proportion of mullite ($3\text{Al}_2\text{O}_3 \cdot 2\text{SiO}_2$) calculated from the chemical analysis results (Table 2), on a calcined basis if all the Al_2O_3 is forming mullite, is ~ 38.9 wt.%. It follows from these results that some mullite crystals have been attacked and dissolved by the vitreous phase as increasing firing temperatures.

It must be noted that the vitreous phase is an undercooled liquid at high temperatures [5,38,39,53,54] and almost the oxides distinct of silica and alumina (Table 2) are forming this phase. In the case of clay-based ceramics such as triaxial whiteware bodies, the melting feldspars dissolves fine quartz grains, increasing the Si content of glassy phase and, hence, its viscosity [54]. Furthermore, it is interesting to remark that a processing approach to synthesize mullite is based in the so-called transient viscous sintering process proposed by Sacks and coworkers [55].

The above considerations are in agreement with the prediction deduced from the $\text{K}_2\text{O}-\text{SiO}_2-\text{Al}_2\text{O}_3$ ternary phase diagram [33,53,56,57]. Thus, the presence of fluxes (see Table 2) influences the thermal behaviour, producing a glassy phase, which is fluid from 985 °C (eutectic). In the thermal study of this pyrophyllite clay, a greater amount of liquid by heating, i.e. glassy phase, will be produced if several components, such as Na_2O , TiO_2 , Fe_2O_3 , CaO and MgO are also present (Table 2), with a total flux content of 4.18 wt.%.

As pointed out in previous studies, the use of sericite as a “natural” flux is interesting because the raw materials with higher sericite content and finer particle size provide very high mullite content at a comparatively low temperature (1000 °C or lower), with improvements in energy savings, as proposed in the literature [32–34].

Interestingly, according with Wang et al. [40], sericite acts both as a sintering additive and a template: it promotes the densification and mullitisation of the matrix and the formation of mullite crystals in these ceramics. They are very interesting findings in accordance with precedent reports and the results obtained in the present investigation.

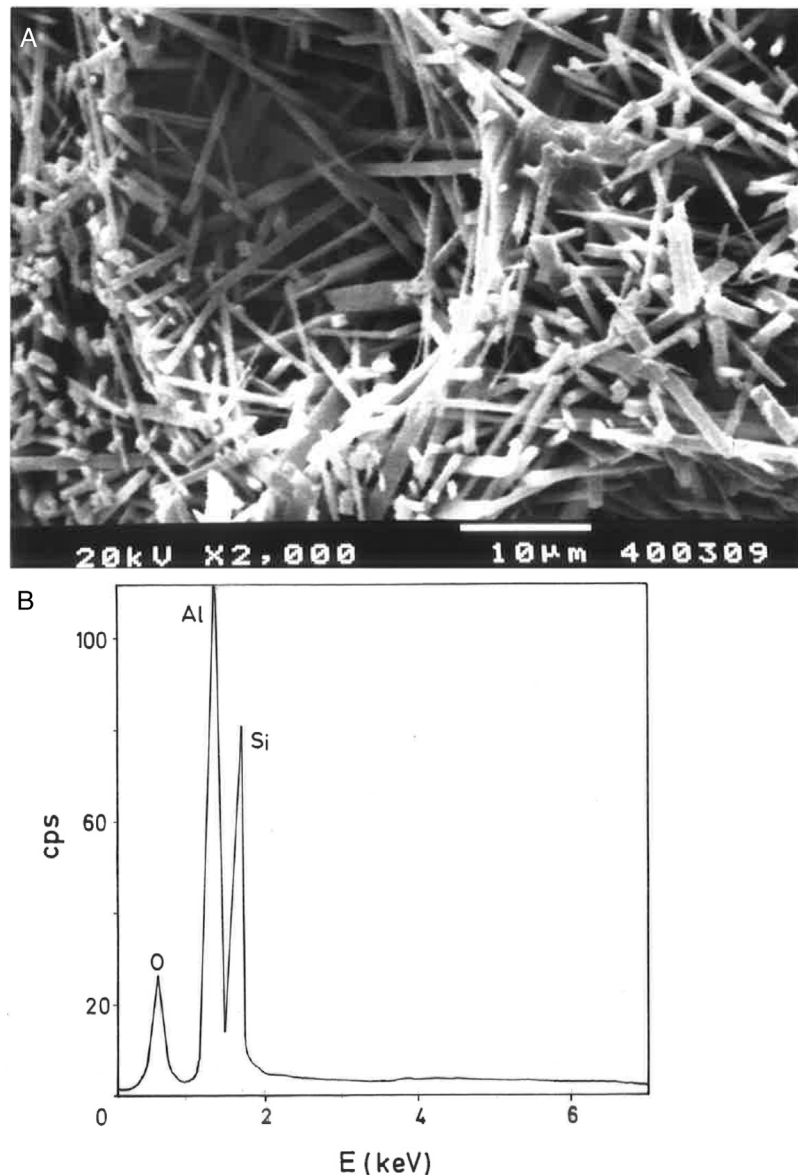


Fig. 8 – Selected SEM micrograph of the pyrophyllite clay sample fired at 1300 °C for 1 h after chemical etching (a) using aqueous HF (20 wt.%) and the corresponding EDS analysis (b) of this sample.

Conclusions

In this work, it has been investigated the sintering behaviour of a pyrophyllite clay, which can be also considered as a sericite clay containing pyrophyllite and kaolinite. A previous mineralogical, textural and chemical characterisation of the studied clay sample indicated that more than 80 wt.% of grain size is minor of 50 μm, with ~22 wt.% of clay fraction. The mineralogical composition, deduced by XRD, showed ~35 wt.% pyrophyllite, ~25 wt.% sericite/illite, ~15 wt.% kaolinite and ~20 wt.% quartz as the main crystalline phase minerals. The chemical composition was consistent with these results showing a total flux content of 4.18 wt.%.

Sintering diagrams using dry pressed ceramic bodies were obtained using the results of linear firing shrinkage, water absorption capacity, bulk density and apparent porosity

determined in the ceramic bodies as a function of firing temperatures (800–1500 °C, with 0.5–5 h of soaking times). The temperature of maximum bulk density was ~1200 °C and the vitrification temperature was ~1300 °C where the apparent porosity becomes almost zero. A trend of slight bulk density values was observed for the bodies fired in the range 1000–1150 °C each 50 °C, with marked decreases of these values for samples fired at 1200 °C and 1300 °C.

The vitrification process of the pyrophyllite clay, as a first approximation, was studied using a method previously described in the literature for kaolinitic samples [2,3], which considered an Arrhenius approach under isothermal conditions and a first order kinetic. In the present study, it was determined an exponential factor or ratio $E_a/R = 5.422$ being $E_a \sim 45 \text{ kJ/mol}$, with a correlation coefficient of 0.998 following the Arrhenius plot. The relative rates of vitrification, or degree of vitrification attained during soaking period, were

calculated. It was determined the overall degree of vitrification attained during heat the main treatment of the pyrophyllite clay body according to a fixed firing schedule. It was found that the contribution of vitrification due to the heating of this pyrophyllite clay sample was relatively small compared to the vitrification during soaking. Then, it was remarked that the vitrification rate equation could be a useful tool to calculate the optimum firing conditions of this pyrophyllite clay.

Further analysis of crystalline and vitreous phases produced after firing allowed to conclude that mullite and quartz are the main crystalline phases of the ceramic bodies, besides a vitreous or glassy phase. Mullite was formed by decomposition of the phyllosilicates present in the clay sample (pyrophyllite, kaolinite and sericite/illite). Quartz was already present in the original sample. It was estimated a relative proportion of crystalline (mullite + quartz) and vitreous phases of $\sim 1:1$ by firing the sample at $1300^{\circ}\text{C}/1\text{h}$, with $\sim 34 \pm 2$ wt.% of mullite crystals as determined by gravimetry (using aqueous HF as chemical agent to eliminate quartz and the glassy phase).

SEM observations of heated pyrophyllite clay samples showed a dense network of rod-shaped and elongated needle-like crystals, being characteristic features of mullite as a dense felt. It is an advantage when pyrophyllite clays with sericite are applied as ceramic raw materials. In accordance with previous findings, the presence of sericite in this pyrophyllite clay promoted the crystallisation of mullite and the densification of the ceramic matrix.

It can be concluded that the research and results presented in this work will contribute to a better knowledge of the characteristics of thermal behaviour and sintering of pyrophyllite clays, applied mainly as ceramic raw materials, and looking for the optimum firing conditions. Next step of research will be the study of sintering behaviour under industrial firing conditions.

Acknowledgements

The authors want to dedicate this paper to the memory of Dr. Celia Maqueda Porras, Research Professor of CSIC (National Spanish Research Council) at the IRNAS, CSIC, Sevilla, for her contribution to the analytical studies and investigations on raw pyrophyllite clays along years. This work was supported by "Junta de Andalucía" through Research Groups TEP 204 and AGR107. Thanks are extended to Alicún Prospecciones S.L. for provide the sample.

REFERENCES

- [1] A.W. Norris, D. Taylor, I. Thorpe, Range curves: an experimental method for the study of vitreous pottery bodies, *Br. Ceram. Trans.* **J.** *78* (1979) 102–108.
- [2] V.T.L. Bogahawatta, A.B. Poole, Estimation of optimum firing conditions for kaolinitic clay bodies, *Br. Ceram. Trans.* **J.** *90* (1991) 52–56.
- [3] S.M. Faieta-Boada, I.J. McColm, Preliminary analysis of the thermal behavior of an industrially used Ecuadorian clay, *Appl. Clay Sci.* **8** (1993) 215–230.
- [4] J. James, S. Rao, Characterization of silica in rice husk ash, *Am. Ceram. Soc. Bull.* **65** (1986) 1177–1180.
- [5] A. Khalfaoui, S. Kacim, M. Hajjaji, Sintering mechanism and ceramic phases of an illitic-chloritic raw clay, *J. Eur. Ceram. Soc.* **26** (2006) 161–167.
- [6] T. Tarvornpanich, G.P. Sousa, W.E. Lee, Microstructural evolution in clay-based ceramics. I. Single components and binary mixtures of clay, flux and quartz filler, *J. Am. Ceram. Soc.* **91** (2008) 2264–2271.
- [7] T. Tarvornpanich, G.P. Sousa, W.E. Lee, Microstructural evolution in clay-based ceramics. II. Ternary and quaternary mixtures of clay, flux and quartz filler, *J. Am. Ceram. Soc.* **91** (2008) 2272–2280.
- [8] R.A. Silva, S.R. Teixeira, A.E. Souza, D.I. Santos, M. Romero, J.M. Rincón, Nucleation kinetics of crystalline phases from a kaolinitic body used in the processing of red ceramics, *Appl. Clay Sci.* **52** (2011) 165–170.
- [9] S.N. Monteiro, C.M.F. Vieira, Solid state sintering of red ceramics at lower temperatures, *Ceram. Int.* **30** (2004) 381–387.
- [10] W.D. Kingery, H.K. Bowden, D.R. Uhlmann, *Introduction to Ceramics*, 2nd ed., Wiley-Interscience, New York, 1976.
- [11] S. Freyburg, A. Schwarz, Influence of the clay type on the pore structure of structural ceramics, *J. Eur. Ceram. Soc.* **27** (2007) 1727–1733.
- [12] D. Wattanasiriwech, K. Srijan, S. Wattanasiriwech, Vitrification of illite clay from Malaysia, *Appl. Clay Sci.* **43** (2009) 57–62.
- [13] V. Melnick, S.A. Pianaro, S. Cava, S.M. Tebcherani, Application of oil shale mining by-products as raw materials in the determination of the vitrification curve of red porcelain stoneware tiles by dilatometric method, *Appl. Clay Sci.* **50** (2010) 311–314.
- [14] G.L. Lecomte-Nana, J.P. Bonnet, P. Blanchart, Investigation of the sintering mechanism of kaolin-muscovite, *Appl. Clay Sci.* **51** (2011) 445–451.
- [15] R.H.S. Robertson, Industrial uses of clay minerals, *Silic. Ind.* **38** (1973) 33–43.
- [16] V.V. Zaykov, V.N. Udachin, Pyrophyllite and pyrophyllite raw materials in the sulfide-bearing areas of the Urals, *Appl. Clay Sci.* **8** (1994) 417–435.
- [17] P.J. Sánchez-Soto, J.L. Pérez-Rodríguez, Características generales, propiedades, yacimientos y aplicaciones de pirofilita. I. Estructura, síntesis y características térmicas, *Bol. Soc. Esp. Ceram. Vidr.* **37** (1998) 279–289.
- [18] P.J. Sánchez-Soto, J.L. Pérez-Rodríguez, Características generales, propiedades, yacimientos y aplicaciones de pirofilita. II. Yacimientos, aplicaciones y utilización como materia prima cerámica, *Bol. Soc. Esp. Ceram. Vidr.* **37** (1998) 359–368.
- [19] A. Bentayeb, O. Masson, Y. Noack, A. Yacoubi, A. Nadiri, A mineralogical study of a natural pyrophyllite, *Powder Diff.* **15** (2000) 51–55.
- [20] A. Bentayeb, M. Amouric, J. Olives, A. Dekayir, A. Nadiri, XRD and HRTEM characterization of pyrophyllite from Morocco and its possible applications, *Appl. Clay Sci.* **22** (2003) 211–221.
- [21] P.J. Sánchez-Soto, M.C. Jiménez, J. Pascual, M. Raigón, J.L. Pérez-Rodríguez, Influence of mechanical and thermal treatments on raw materials containing pyrophyllite, *Bol. Soc. Esp. Ceram. Vidr.* **39** (2000) 119–134.
- [22] E.W. Emrich, Use of high-sericite pyrophyllite in vitreous bodies, *J. Am. Ceram. Soc.* **24** (1941) 141–144.
- [23] T.K. Mukhopadhyay, S. Ghosh, S. Ghatak, H.S. Maiti, Effect of pyrophyllite on vitrification and on physical properties of triaxial porcelain, *Ceram. Int.* **32** (2006) 871–876.
- [24] T.K. Mukhopadhyay, S. Ghatak, H.S. Maiti, Effect of pyrophyllite on the mullitization in triaxial porcelain system, *Ceram. Int.* **35** (2009) 1493–1500.

- [25] T.K. Mukhopadhyay, S. Ghatak, H.S. Maiti, Pyrophyllite as raw material for ceramic applications in the perspective of its pyro-chemical properties, *Ceram. Int.* 36 (2010) 909–916.
- [26] A. Talidi, N. Saffaj, K.E. Kacemi, S.A. Younssi, A. Albizane, A. Chakir, Processing and characterization of tubular ceramic support for microfiltration membrane prepared from pyrophyllite clay, *Sci. Stud. Res.: Chem. Eng. Biotechnol. Food Ind.* 12 (2011) 263–268.
- [27] J.-H. Ha, J. Lee, I.-H. Song, S.-H. Lee, The effects of diatomite addition on the pore characteristics of a pyrophyllite support layer, *Ceram. Int.* 41 (2015) 9542–9548.
- [28] J.-H. Ha, S. Lee, S.Z. Bukhari, J. Lee, I.H. Son, The preparation and characterization of alumina-coated pyrophyllite-diatomite composite support layers, *Ceram. Int.* 43 (2017) 1536–1542.
- [29] I. González, P. Campos, C. Barba-Brioso, A. Romero, E. Galán, E. Mayoral, A proposal for the formulation of high-quality ceramic “green” material with traditional raw materials mixed with Al-clays, *Appl. Clay Sci.* 131 (2016) 113–123.
- [30] S. Ferrari, A.F. Gualteri, The use of illitic clays in the production of stoneware tile ceramics, *Appl. Clay Sci.* 32 (2006) 73–81.
- [31] E. Galán Huertos, J.J. Martín Vivaldi, Caolines españoles. Geología, mineralogía y génesis. Parte 6, *Bol. Soc. Esp. Ceram. Vidr.* 13 (1974) 523–546.
- [32] J. Espinosa de los Monteros, M.A. Del Río, R. Martínez-Cáceres, D. Alvarez-Estrada, V. Aleixandre, Sericite clay as a raw material for the fabrication of whitewares bodies, *Ceram. Int.* 3 (1977) 109–114.
- [33] J. Espinosa de los Monteros, D. Alvarez Estrada, F. Morales Poyato, M.A. Del Río Sánchez, Arcillas sericíticas. Nuevas materias primas cerámicas, *Bol. Soc. Esp. Ceram. Vidr.* 17 (1978) 73–78.
- [34] J. Espinosa de los Monteros, D. Alvarez-Estrada, R. Martínez, Porcelanas aluminosas de elevada resistencia mecánica obtenidas a partir de arcillas sericíticas, *Bol. Soc. Esp. Ceram. Vidr.* 18 (1979) 11–16.
- [35] J.M. Rincón, Rocas y minerales de Extremadura como posibles materias primas en la producción de vidrios y materiales cerámicos. Materiales cerámicos y vítreos, in: Los materiales cerámicos y vítreos en Extremadura, edición UNED y SECV, Mérida, 1988, pp. 135–158.
- [36] J.M. Mesa López-Colmenar, Contribución al estudio mineralógico de las Pizarras Alumínicas (Tierras Blancas) del Paleozoico de la provincia de Badajoz, Tesis Doctoral, Universidad de Sevilla, 1986.
- [37] P.J. Sánchez-Soto, A. Justo, M.C. Jiménez de Haro, J.L. Pérez-Rodríguez, M. Raigón, J. Pascual, Caracterización y propiedades cerámicas de una pizarra alumínica que contiene pirofilita, *Bol. Soc. Esp. Ceram. Vidr.* 33 (1994) 199–205.
- [38] F. González-Miranda, E. Garzón, J. Reca, L. Pérez-Villarejo, S. Martínez-Martínez, P.J. Sánchez-Soto, Thermal behavior of sericite clays as precursors of mullite materials, *J. Therm. Anal. Calorim.* 132 (2018) 967–977.
- [39] P.J. Sánchez-Soto, D. Eliche-Quesada, S. Martínez-Martínez, E. Garzón, L. Pérez-Villarejo, J. Ma Rincón, The effect of vitreous phase on mullite and mullite-based ceramic composites from kaolin wastes as by-products of mining, sericite clays and kaolinite, *Mater. Lett.* 223 (2018) 154–158.
- [40] X. Wang, J.-H. Li, W.-M. Guan, M.-J. Fu, L.-J. Liu, Emulsion-templated high porosity mullite ceramics with sericite induced textural structures, *Mater. Des.* 89 (2016) 1041–1047.
- [41] Y.-H. Hsiao, T.-Y. Ho, Y.-H. Shen, D. Ray, Synthesis of analcime from sericite and pyrophyllite by microwave-assisted hydrothermal processes, *Appl. Clay Sci.* 143 (2017) 378–386.
- [42] E. Galán Huertos, J. Espinosa de los Monteros, El caolín en España, in: Características, identificación y ensayos cerámicos, Ed. Sociedad Española de Cerámica y Vidrio, Madrid, 1975.
- [43] R. Sule, I. Sigalas, Effect of temperature on mullite synthesis from attrition-milled pyrophyllite and α -alumina by spark plasma sintering, *Appl. Clay Sci.* 162 (2018) 288–296.
- [44] J.L. Pérez-Rodríguez, C. Maqueda, A. Justo, Pyrophyllite determination in mineral mixtures, *Clays Clay Miner.* 33 (1985) 563–566.
- [45] C. Maqueda, J.L. Pérez-Rodríguez, A. Justo, Problems in the dissolution of silicates by acid mixtures, *Analyst* 111 (1986) 1107–1108.
- [46] L.G. Schultz, Quantitative interpretation of mineralogical composition from X-ray and chemical data for the Pierre Shale. U.S. Geol. Surv. Professional Papers, 1964, pp. 391C.
- [47] P.E. Biscaye, Mineralogy and sedimentation of recent deep-sea clay in the Atlantic Ocean and adjacent sea and oceans, *Geol. Soc. Am. Bull.* 76 (1965) 803–831.
- [48] G. García-Ramos, F. González-García, P.J. Sánchez-Soto, M.T. Ruiz-Abrio, Propiedades refractarias y studio de los productos obtenidos a partir de un conjunto de materiales silicoaluminosos españoles. I, *Bol. Soc. Esp. Ceram. Vidr.* 24 (1985) 67–79.
- [49] S.A.T. Redfern, The kinetics of dehydroxylation of kaolinite, *Clay Miner.* 22 (1987) 447–456.
- [50] A. Wiewióra, P.J. Sánchez-Soto, M.A. Avilés, A. Justo, J.L. Pérez-Rodríguez, Effect of dry grinding and leaching on polytypic structure of pyrophyllite, *Appl. Clay Sci.* 8 (1993) 261–282.
- [51] M.P. Riccardi, B. Messiga, P. Duminuco, An approach to the dynamics of clay firing, *Appl. Clay Sci.* 15 (1999) 393–409.
- [52] I.A. Aksay, D.M. Dabbs, M. Sarikaya, Mullite for structural, electronic and optical applications, *J. Am. Ceram. Soc.* 74 (1991) 2343–2354.
- [53] G.L. Lecomte, B. Pateyron, P. Blanchart, Experimental study and simulation of a vertical section mullite-ternary eutectic (985 °C) in the $\text{SiO}_2\text{--Al}_2\text{O}_3\text{--K}_2\text{O}$ system, *Mater. Res. Bull.* 39 (2004) 1469–1478.
- [54] W.E. Lee, G.P. Sousa, C.J. McConville, T. Tarvornpanich, Y. Iqbal, Mullite formation in clays and clay-derived vitreous ceramics, *J. Eur. Ceram. Soc.* 28 (2008) 465–471.
- [55] M.D. Sacks, N. Bozkurt, G.W. Scheiffele, Fabrication of mullite and mullite-matrix composites by transient viscous sintering of composite powders, *J. Am. Ceram. Soc.* 74 (1991) 2428–2437.
- [56] E.F. Osborn, A. Muan (Eds.), Phase Diagrams for Ceramists. Plate 407, American Ceramic Society, Columbus, OH, USA, 1960.
- [57] K.C. Liu, G. Thomas, A. Caballero, J.S. Moya, S. De Aza, Time-temperature-transformation curves for kaolinite- α -alumina, *J. Am. Ceram. Soc.* 77 (1994) 1545–1552.